

Research Article

Potential Revenue from Reserve Market Participation in Wind Power- and Solar Power-Dominated Electricity Grids: The Near-Term, Mid-Term, and Long-Term

Jonathan Ullmark , Lisa Göransson , and Filip Johnsson 

Department of Space, Earth and Environment, Energy Technology, Chalmers University of Technology, Gothenburg, Sweden

Correspondence should be addressed to Jonathan Ullmark; jonathan.ullmark@chalmers.se

Received 14 August 2023; Revised 4 December 2023; Accepted 22 January 2024; Published 22 February 2024

Academic Editor: Yashwant Sawle

Copyright © 2024 Jonathan Ullmark et al. This is an open access article distributed under the Creative Commons Attribution License, which permits unrestricted use, distribution, and reproduction in any medium, provided the original work is properly cited.

As electricity systems become increasingly dominated by variable inverter-based generation (such as wind and solar photovoltaics (PV)), additional sources of variability appear, while the share of dispatchable thermal power plants decreases. Maintaining a stable grid frequency requires new sources of inertia to slow the frequency changes, as well as new sources of reserve power to counter the imbalances. This work uses a linear optimization modeling approach to analyze the reserve market of the electricity system during the transition to a carbon-free system with high shares of variable electricity generation. The modeling is performed for three regional contexts and with varying degrees of available flexibility technologies. As for the reserve supply, batteries, electrolyzers, electric boilers and heat pumps for district heating, curtailed wind and solar power, and hydropower and thermal power plants are all included. The results indicate that of these suppliers of reserves, the introduction of grid-scale batteries into the system drastically reduces the reserve market size. Only early in the transition is revenue from the reserve market greater than 5% of the total revenue for any technology. While the demand for reserves increases as the share of solar PV and wind power increases, the modeling reveals that access to flexible loads, storage units, and emulated inertia from wind power also increases. Depending on the choice of flexibility measures available, demand-side participation could play a major role in minimizing the cost of grid stability in the future.

1. Introduction

The ongoing transition of electricity generation from systems dominated by traditional thermal power plants to systems with higher shares of variable renewable energy (VRE), such as wind and solar power, is creating challenges for the physical electricity system, the immaterial markets, and the grid codes that facilitate the efficient operation of the electricity system. *Inertia*, which is often available at no additional cost in traditional systems, may require market incentivization or forced support from inverter-based generators and storage through the grid code. *Reserve power* may be in higher demand as more

variations are introduced to the system, and the categorization of reserve supply may have to change so as to accommodate more effectively the technical properties of potential new reserve suppliers, such as batteries, wind power, and solar PV. Both the current and future actors in the electricity systems have a vested interest in the structure of the future markets and grid codes, and they will benefit from information regarding how their revenue streams may change during the energy transition.

Potential revenue and reserve power market developments are fields of interest for research. Previous studies on these topics have included comparisons of methodologies to predict electricity markets [1] and evaluate bidding

strategies ([2–4]), and studies that have examined the roles and revenues of various potential reserve suppliers ([2, 5–16]). Merten et al. [1] have compared both statistical and machine learning models for the purpose of predicting the market price for automatic frequency restoration reserves (aFRRs) in continental Europe, finding no clear winner among the models. Nitsch et al. [2] have simulated day-ahead and aFRR markets to delineate the potential revenues for batteries, finding that the total revenue increases in the year 2030 scenario (with 60% of electricity from renewable sources), as compared to the year 2019, and that the day-ahead revenue share increases relative to the reserve revenue. Merten et al. [3] have also found that the total simulated revenue increases in Germany in the near future (year 2025), while the reserve share decreases. Badedo et al. [4] have used agent-based market simulations to investigate how the frequency containment reserve (FCR) market could develop as the electricity system transitions towards higher shares of renewable energy and increasing battery capacities. However, to the best of our knowledge, no studies have included frequency control support from a wider range of technologies, including demand-side technologies (power-to-heat and power-to-H₂), generation-side technologies (thermal, hydro, wind, and solar power), and storage technologies (batteries and hydrogen storage units).

To understand the roles and values of specific technologies in the electricity grid, one can optimize the electricity system to identify the technology mix that can supply the demand for electricity (and for other possible products within the energy system) at the least cost. Generation expansion planning (GEP) models do this for electricity generation systems [17–23], covering the range from regional or national analysis to international or even continental scopes. These electricity system optimization models often include all or some of the following: limited transmission between multiple copper-plate regions; new investments in generation, storage, and transmission capacity; flexibility limitations in relation to thermal power plants; and exogenous generation profiles for wind and solar power. The outputs from these models include cost-optimal investments and operation of each technology, as well as the resulting electricity prices, CO₂ emissions levels, and electricity exchanges between regions. A representation of the inertia and reserve power demand in each region can also be included (as in, for example, [24–30]), either to improve the feasibility of the resulting system or to investigate the impacts of the inertia and reserve power demand on the system composition, cost, and operation. By analyzing suppliers of inertia and power reserves in an optimized electricity system, interactions between technologies and between different markets can be captured. van Stiphout et al. [30] have studied the impact of including a reserve demand in investment planning of an electricity system that consists of base-, mid-, and peak-generation, as well as varying shares of PV and wind power. However, their model does not include any storage technologies or flexible demand. They have shown that including a reserve demand can significantly influence the total system cost and system

composition, although this impact is weakened if wind and solar PV are allowed to provide downward reserves. González-Inostroza et al. [26] have investigated the roles of energy storage in providing fast frequency reserves in Chile for the year 2050 and have found that the reserve supply from inverter-based technologies, such as batteries, is critical for achieving secure operation of a fully renewable electricity system. However, their model includes only one decarbonized future year and thus gives no insights into the transition to this decarbonized future. A previous study conducted by the authors of the present work [31] examined the interactions between generation and storage technologies for the electricity supply, as well as technologies to supply inertia and reserves, focusing on the impacts on the system cost and composition. They have shown that flexibility from storage units, including flexibly charging EVs, plays an important role in limiting the impacts of grid frequency control on the system cost and composition. However, none of these studies has specifically investigated how the reserve markets might develop during the energy transition or the potential revenue for individual technologies participating in the reserve market. There is thus a gap in the research field regarding which markets may drive investments in technologies providing frequency control, as well as at which point of the energy transition these investments are desired. Therefore, this work investigates how the revenue from markets for frequency reserves can change over time for different technologies participating in electricity generation and the provision of reserves.

2. Methodology

This work is based on linear optimization modeling, using a model described in the thesis of Ullmark [32]. The model optimizes investments and usage of transmission lines, generation, and storage to minimize the total system cost. At the same time, sufficient inertia and reserves must be available for every hour. Each modeled hour is split into six intrahourly intervals, with the first one starting at 1 second following an imbalance (activation time, 1 second) and the last one ending at 60 minutes, at which point a new time-step is active with new interhourly intervals and reserves, which must be available. The division of intrahourly intervals is shown in the header of Table 1, where the length and activation speed of each interval are included. Figure 1 illustrates, in simplified form, the technologies that contribute to the frequency reserve supply in this work. A more detailed mathematical description of the model can be found in Section 2.1.

The mathematical model is applied to the three regional cases illustrated in Figure 2, each with interconnected subregions and different wind and solar profiles and resources. The hydro reservoir inflow, as well as the load, run-of-river, wind, and solar profiles, are based on historical data from the year 2012, which was a typical year for these aspects. The scenarios and parameters used are described in more detail in Section 2.2.

In Figure 3, an overview of the model setup is shown, illustrating how the optimization model interacts with a

TABLE 1: Shares of each reserve demand source active in each intrahourly interval.

	1–5 s	5–30 s	30 s–5 min	5–15 min	15–30 min	30–60 min
$N - 1$	1	1	1	1	1	1
VRE ramping	0	0	0	1	1	1
Stochastic load variations	0	0.08	0.39	0.99	1	1

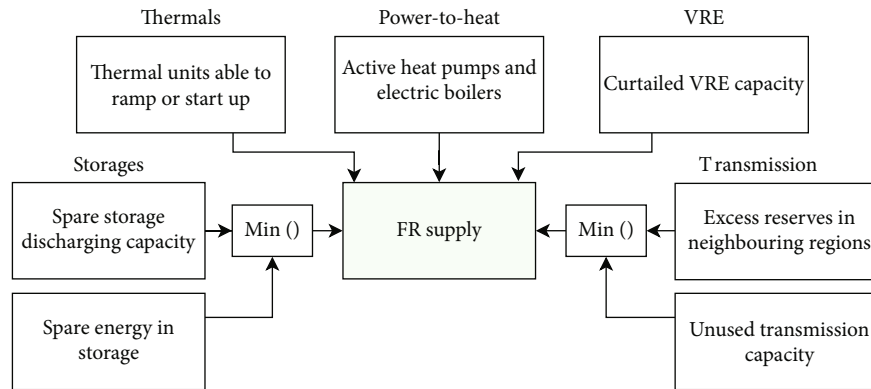


FIGURE 1: Schematic of the various FR supply sources. The storage units considered in this work are batteries and hydrogen caverns. Source: [31].

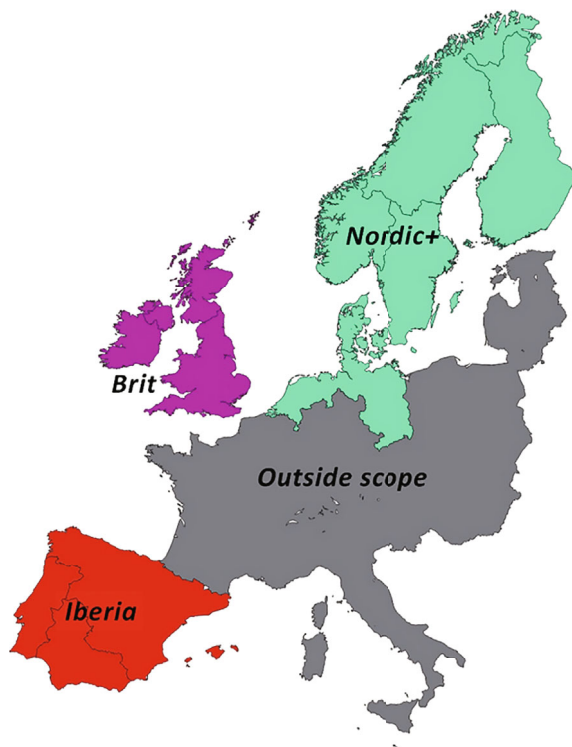


FIGURE 2: Map of part of Europe illustrating the three regional cases applied in this work with respect to existing generation and transmission capacities, VRE potentials and generation profiles, and electricity loads and load profiles. Brit: England + Wales, Scotland, Northern Ireland, and Ireland; Iberia: northeastern Spain, southwestern Spain, and Portugal; Nordic: Finland, northern Sweden + northern Norway, southern Norway, southern Sweden + eastern Denmark, and Netherlands + western Denmark + northeastern Germany.

Python script to forward investments made during one modeled year to the next. This setup enables the modeling of stages along a transition from the existing real-world system towards a future carbon-neutral system, with separate investment decisions made at each stage.

2.1. Mathematical Model. The linear optimization model used in this work was originally developed by Göransson et al. [33], and thereafter extended by Johansson and Göransson [34] to include additional flexibility measures, and then by Ullmark et al. [31] to include multiple years and the demand for inertia and reserves. The model features both long- and short-term storage units, preexisting (real-life) generating and transmission capacities, and new investments in storage, transmission, and generating capacity. Table 2 lists the sets, variables, and parameters used in the equations describing the model.

The objective function to be minimized is the total system cost shown in Eq. (1). The variables in Eq. (1) are storage and generating investments ($i_{r,p}$) in subregion r and technology p , transmission capacity investments ($i_{r,r',b}^{\text{tran}}$) in transmission technology b from subregion r to subregion r' , and generation ($g_{r,t,p}$) of technology p in subregion r for time-step t . For thermal power plants, thermal cycling is implemented linearly through a distinction between online thermal capacity ($g_{r,t,p}^{\text{active}}$) and active power output ($g_{r,t,p}$). This implementation allows for start-up and part-load costs, as well as part-load emissions, and is described in detail by Göransson et al. [33] and based on a book by Weber [35]. Real existing power capacity is combined with investments made in previous model years (if any) to create a homogeneous level of preexisting capacity for each technology type (except for storage). This is expressed as $g_{r,t,p}^{\text{existing}}$ and

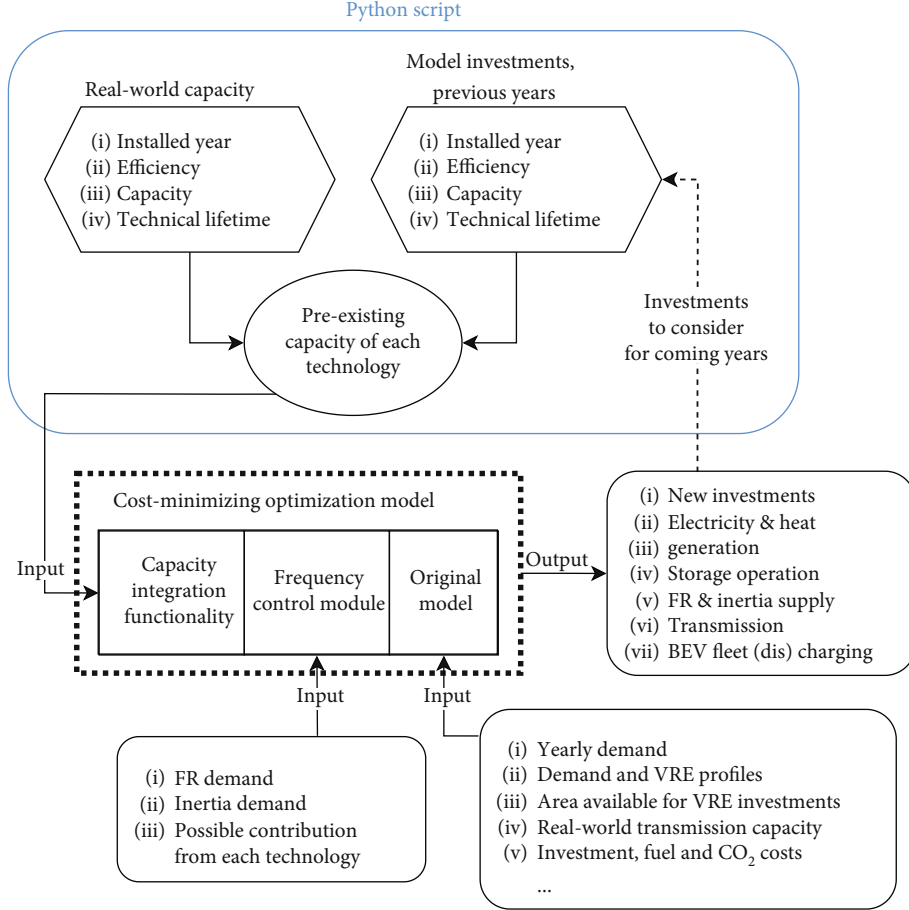


FIGURE 3: Illustration of the model setup enabling multiple modeled years along a transition from the current system to a future carbon-neutral electricity generation system.

differs from new capacity due to efficiency improvements made over time.

$$\begin{aligned}
 \min \sum_{r \in R} \left(\sum_{p \in P} i_{r,p} * C_p^{\text{inv}} + \sum_{r', b \in R, B} i_{r,r',b}^{\text{tran}} * C_{r,r',b}^{\text{trans}} \right. \\
 + \sum_{t,p \in T, P^{\text{gen}}} \left(g_{r,t,p} * C_p^{\text{OPEX}} + g_{r,t,p}^{\text{existing}} * C_p^{\text{existing,OPEX}} \right) \\
 + \sum_{p \in P} i_{r,p} * C_p^{\text{fixOM}} + \sum_{t,p \in T, P^{\text{gen}}} \left((g_{r,t,p}^{\text{active}} - g_{r,t,p}) * C_p^{\text{part}} \right. \\
 + \left. (g_{r,t,p}^{\text{existing,active}} - g_{r,t,p}^{\text{existing}}) * C_p^{\text{existing,part}} \right) \\
 \left. + \sum_{t,p \in T, P^{\text{gen}}} \left(g_{r,t,p}^{\text{start}} * C_p^{\text{start}} + g_{r,t,p}^{\text{existing,start}} * C_p^{\text{existing,start}} \right) \right). \quad (1)
 \end{aligned}$$

Storage units are balanced on a regional basis, as shown in Eqs. (2) and (3). Equation (2) describes the hour-to-hour balance of storage systems, and Eq. (3) describes the charge and discharge limitations from the installed (dis)charge capacity and the (dis)charge rate limits specific to the storage type. In these equations, $s_{r,t,p}^{(\text{dis})\text{charge}}$ indicates the amount of

energy coming in or out of the storage, $g_{r,t,p}$ indicates the storage level, and $E_{r,q}$ is the preexisting capacity of the (dis)charge technology q and subregion r .

$$\begin{aligned}
 g_{r,t+1,p} = g_{r,t,p} + s_{r,t,p}^{\text{charge}} * \eta_p^{\text{ESS}} - \frac{s_{r,t,p}^{\text{discharge}}}{\eta_p^{\text{ESS}}}, \forall r, t, p \in R, T, P^{\text{ESS}}, \quad (2) \\
 -(i_{r,p} + E_{r,p}) * S_p^{\text{rate}} \leq -i_{r,q^{\text{in}}} - E_{r,q^{\text{in}}} \leq s_{r,t,p}^{\text{discharge}} - s_{r,t,p}^{\text{charge}} \\
 \leq i_{r,q^{\text{out}}} + E_{r,q^{\text{out}}} \leq (i_{r,p} + E_{r,p}) \\
 * S_p^{\text{rate}}, \forall r, t, (p, q^{\text{in}}, q^{\text{out}}) \in R, T, Q. \quad (3)
 \end{aligned}$$

Between these subregions, existing and new transmission capacities allow for the trading of electricity according to Eqs. (4)–(6). Equations (4) and (5) ensure symmetry between import and export between any pair of subregions, and Eq. (6) limits transmission to the total transmission capacity.

$$i_{r,r',p}^{\text{tran}} = -i_{r',r,p}^{\text{tran}}, \forall r, r', p \in R, R, P^{\text{trans}}, \quad (4)$$

TABLE 2: Sets, variables, and parameters used in the mathematical description of the model.

Sets		
B	Electricity transmission technologies (OHAC and HVDC)	
R	Subregions	
T	Time-step, $\{1,..,8784\}$	
P	Technology	
P^{VRE}	Variable renewable technologies (wind, solar, and run-of-river)	
$P^{inertia}$	Technologies able to provide inertia (wind power and synchronous generators)	
P^{FR}	Technologies able to provide frequency reserves	
P^{ESS}	Energy storage technologies (Li-ion batteries and hydrogen storage)	
P^{charge}	Energy storage charging technologies	
$P^{discharge}$	Energy storage discharging technologies	
P^i	Electricity-generating technologies	
O	Frequency reserve interval $\{1,..,6\}$	
Q	$P^{ESS} \times P^{charge} \times P^{discharge}$ matrix connecting energy storage units with their respective charging capacity technologies (e.g., electrolyzer and inverter) and discharge capacities	
Variables		
$e_{r,r',t}^{netexport}$	Electricity net export from region r to region r' during time-step t	GWh/h
$i_{r,p}$	Investment in technology p in region r	GW
$g_{r,t,p}$	Generation, or storage level, for technology p at time-step t in region r	GWh/h
$s_{r,t,p}^{charge}$	Charging of storage p in region r at time-step t	GWh/h
$s_{r,t,p}^{discharge}$	Discharging of storage p in region r at time-step t	GWh/h
$as_{r,t,p}^{inertia}$	Available inertial power	GW
$as_{r,t,p,o}^{FR}$	Available frequency reserves	GW
Parameters		
η_p^{ESS}	Charging and discharging efficiency of technology p	-
A_o	Equals 1 for frequency reserve intervals o 3–6, for which VRE variations cause a reserve demand	-
C_p^{inv}	Investment cost for technology p	k€/GW
C_p^{OPEX}	Running cost (including fuel, CO ₂ , and variable O&M costs) for technology p	k€/GWh
C_p^{fixOM}	Fixed yearly O&M cost for technology p	
C_p^{start}	Start-up cost for technology p	k€/GW
C_p^{part}	Part-load cost for technology p	k€/GW
$E_{r,p}$	Already existing capacity of technology p in region r	GW(h)
$E_{r,r',p}^{trans}$	Already existing transmission capacity of technology p between regions r and r'	GW
$I_{r,t}^{load}$	Frequency reserve demand due to intrahourly load variations	GW
I_r^{N-1}	Frequency reserve demand to cover for worst single fault ($N - 1$)	GW
I^{dur}	Duration of inertia power response (10 s)	s
I_p^{power}	Inertial power response from connected generators (see Table 4)	-
$O_{p,o}^{on}$	Ability of technology p to increase output until reserve interval o	-
$O_{p,o}^{off}$	Ability of technology p to start up until reserve interval o	-

TABLE 2: Continued.

O_o^{dur}	Duration of reserve window o	s
S_p^{rate}	Storage (dis)charge rate as a fraction of storage per hour	[-]
$W_{t,p}$	Hourly profile for VRE (equal to 1 for dispatchable technologies)	[-]

OHAC: over-head, alternating current; HVDC: high-voltage, direct current; O&M: operation and maintenance.

$$e_{r,r',t}^{\text{netexport}} = -e_{r',r,t}^{\text{netexport}}, \forall r, r', t \in R, R, T, \quad (5)$$

$$-\left(i_{r,r',p}^{\text{tran}} + E_{r,r',p}^{\text{trans}}\right) \leq e_{r,r',t}^{\text{netexport}} \leq i_{r,r',p}^{\text{tran}} + E_{r,r',p}^{\text{trans}}, \forall r, r', t, p \in R, R, T, P^{\text{trans}}. \quad (6)$$

Equations (7) and (8) make up part of the frequency reserve and inertia implementation. Equation (7) describes the inertia demand balance, which involves the total synchronous inertia from thermal and hydropower plants, and the synthetic inertia from flexible power-to-heat and battery storage systems. Similarly, Eq. (8) describes the reserve demand balance, encompassing the total available reserves to meet the demand in each subregion and for each time-step and intrahourly interval. The potential sources of reserves are thermal and hydropower plants and battery and hydrogen storage systems, as well as flexible power-to-heat and hydrogen electrolysis. In this work, the marginal cost of the reserve balance equation is taken as the reserve market price. For a full mathematical description of this implementation, see [31].

$$I_r^{N-1} \leq \sum_{p \in P^{\text{inertia}}} \left((g_{r,t,p}^{\text{active}} + g_{r,t,p}^{\text{existing,active}}) * I_p^{\text{power}} \right) + \sum_{p \in P^{\text{ESS}}} \left(a_{r,t,p}^{\text{inertia,ESS}} \right) + \sum_{p \in P^{\text{PH}}} \left(g_{r,t,p} + g_{r,t,p}^{\text{existing}} \right), \forall r, t \in R, T, \quad (7)$$

$$a_{r,t,o}^{\text{FR}} \geq I_{r,t,o}^{\text{SLV}} + I_r^{N-1} + \sum_{p \in P^{\text{VRE}}} i_{r,p} * \max(W_{r,t,p} - W_{r,t-1,p}, W_{r,t+1,p} - W_{r,t,p}) * O_o^{\text{VRE}}, \forall r, t, o \in R, T, O. \quad (8)$$

2.2. Scenarios and Parameters. The model is applied to three regional cases (illustrated in Figure 2) and two scenarios with different levels of available flexibility (*LowFlex* and *HighFlex*). The differences between the *LowFlex* and *HighFlex* scenarios, and between the three geographic cases, are listed in Table 3.

Both the *LowFlex* and *HighFlex* scenarios include the electricity load from an electrified vehicle fleet, as well as the electricity load from electrified steel, cement, and ammonia production. The implementation for electrified vehicles is adopted from Taljegard et al. [20], using aggregated real driving patterns to build a charging demand and a profile for a number of connected vehicles. No vehicle-to-grid is considered, although it is assumed that 30% of electric vehicles charge strategically. The yearly demands from these new

TABLE 3: Differences between the system flexibility scenarios and geographic cases.

System flexibility scenarios	
HighFlex	30% of the vehicle fleet charging strategically. Transmission capacity and H ₂ storage investments available
LowFlex	30% of the vehicle fleet charging strategically. Only real-world transmission capacity and no H ₂ storage units.
Geographic cases	
Brit	British Isles (Great Britain + Ireland)
Iberia	Iberian Peninsula (Spain + Portugal)
Nordic+	Northern Europe (Sweden + Norway + Finland + Denmark + Netherlands + northern Germany)

TABLE 4: District heating and nontraditional loads (in TWh) from transportation and industry.

	Brit	Iberia	Nordic+
Transport (el.)	1.6/8.2/44/63	1.4/6.9/37/53	1.6/8.1/44/62
Transport (H ₂)	0.1/0.4/2.2/3.2	0.1/0.3/1.9/2.7	0.1/0.4/2.2/3.1
DH (heat)	28/30/32/36	3.5/3.7/4/4.5	120/122/124/128
Steel (el.)	0/0/0.4/2.5	0/0/0.2/1.6	0/0/0.9/5.7
Steel (H ₂)	0/0/0.7/4.5	0/0/0.5/3	0/0/1.7/11
Cement (el.)	0/0/0.5/3	—	0/0/1.4/9
Ammonia (el.)	—	—	0/0/1.8/12

The values shown are for the year 2020/near-term/mid-term/long-term futures.

loads, for each regional case and year/period, are detailed in Table 4. The district heating demand can be supplied using existing or new combined heat and power (CHP) plants or through investments in electric boilers and heat pumps. In addition, the heat load is balanced over 2-week periods, under the implicit assumption that there are heat storage units that confer up to 2 weeks of flexibility on the district heating networks.

The modeled inertia demand is determined by the dimensioning fault in each synchronous grid, divided for each subregion according to the yearly electricity loads, as shown in Table 5. In Table 5, the *Nordic+*, *Brit*, and *Iberia* regions are in italic, bold, and underlined, respectively.

To supply inertia, both synchronous machines and some inverter-based power sources are considered. The inertia constants (H) of synchronous machines are converted into additional power supplied (P) during a dimensioning fault, assuming a rate of change of frequency (RoCoF) of 1.5 Hz/s. Both the inertia constants and inertial power responses

TABLE 5: $N - 1$ values used for each modeled copper-plate subregion.

Subregion	<i>SE + NO N</i>	<i>SE S</i>	<i>NO S</i>	<i>FI</i>	<i>DE N</i>	UK 1	UK 2	UK 3	IE	<u>ES N</u>	<u>ES S</u>	<u>PT</u>
$N - 1$ (GW)	<i>0.08</i>	<i>0.40</i>	<i>0.48</i>	<i>0.37</i>	<i>0.14</i>	0.83	0.08	0.02	0.08	<u>0.16</u>	<u>0.06</u>	<u>0.06</u>

The italic, bold, and underlined data represent the Nordic+, Brit, and Iberia regions, respectively. For an illustration of these regions, see Figure 2.

from the synchronous machines, and wind power, are listed in Table 6. The power response from batteries is limited by the unused net discharging capacity, and the limit for power-to-heat is the currently used capacity.

The dimensioning fault is also combined with the estimated levels of stochastic load variations and intrahourly variations from wind and solar power used to set the reserve demand. Since these different imbalance sources occur with varying degrees of suddenness, they contribute different amounts to the total reserve demand of each inter-hourly reserve interval. The contribution of each source to each interval is listed in Table 1. Reserves to counter the dimensioning fault are required in each interval, starting 1 second after the imbalance and lasting until the next hour. Since the interhourly variations from ramping VRE are known beforehand and ramp up over time, the required reserves have a shorter activation time of 5 minutes. Lastly, the stochastic load variations are not known beforehand but are also not typically appearing suddenly. Their demand for reserves has been assumed to follow the step response from a first-order control system with a time constant of 60 seconds.

A combination of reserve technologies, including both electricity consumers (power-to-heat and electrolyzers for hydrogen consumers) and producers, as well as their activation times, are listed in Table 7. To provide reserves, all storage units are limited by the unused net discharge capacity (as shown in Eq. (3)) and the storage level. In addition, hydropower is limited by the ramping rate listed in Table 7, as are all the online thermal power plants. Offline gas turbine capacity can also contribute, given some time for start-up. In addition to the activation times in Table 7, power-to-heat plants are limited by their current electricity power draw.

2.3. Reserve Revenue and Market Size. To accomplish the aim of this work, to investigate how the revenue from providing reserves changes along the transition and for each technology, the terms *revenue* and *market size* must be defined. Herein, the *reserve revenue* for each technology and hour is assumed to be the reserve price, approximated by the marginal cost of supply (see the reserve demand balance equation, Eq. (8)), and multiplied by the available reserves from the technology. While the numbers found using this method of modeling are not predictors of real market sizes or revenues, they enable comparisons and relative trends in the context of the model. Any margin that is added on top of a technology's cost-to-participate and their market bid is neglected, as if there was perfect competition and no withheld information. The implied market structure to give this reserve price is discussed further in Section 4. The *market size* is calculated by multiplying the reserve price

TABLE 6: Inertia constants and inertial power responses for the different synchronous generator types included in this work. The inertial power response from wind power is based on Imgart and Chen [36].

	Nuclear power	Other thermal	Hydropower	Synchronous condensers	Wind power
H (s)	6	4	3	6	—
ΔP (%)	48	32	24	48	13

by the demand for reserves, summed over each hour, subregion, and reserve interval. As such, the sum of all reserve revenues equals the market size. The system cost of supplying reserves is not presented in this work but is investigated elsewhere by the authors [31].

3. Results

3.1. System Composition. Figure 4 illustrates the transition of the electricity generation from the year 2020 reference system (dispatch-only of the preexisting generation capacity) to a long-term future system, over near-term and mid-term systems. The three regional cases (*Nordic+*, *Brit*, and *Iberia*) are shown, as well as both the *LowFlex* and *HighFlex* scenarios. It is evident that the electricity production levels differ between the regional cases, not only in terms of preexisting generating capacity but also with regard to the final shares of wind, solar, and thermal power. The differences between the *LowFlex* and *HighFlex* scenarios affect the transition mostly in terms of system cost and investments in storage and transmission capacities. As such, the difference between the *LowFlex* and *HighFlex* scenarios shown in Figure 4 is minimal.

The differences between the three regional systems and two flexibility scenarios can also be seen in the generation and storage investments made in each year. Figure 5 shows the investments taken each year in the *LowFlex* scenario (left-hand side) and differences in investments in generation and storage when increasing access to flexibility (*HighFlex* scenario) (right-hand side). For the *Nordic+* case in the *HighFlex* scenario, which allows for investments in hydrogen storage and transmission capacity (not included in the figure), it is clear that the solar PV, electric boiler, and battery storage capacities are reduced. As the hydrogen storage investments and additional transmission to hydropower regions increase, the ability to manage long-term variations increases. This causes some of the solar PV and battery capacities to be displaced, also reducing the solar PV peaks previously used for opportunistic power-to-heat. In the *Brit* region, the battery storage capacity

TABLE 7: For thermal power plants and hydropower plants, the table shows the factor of the rated capacity to which the production can be increased, from part-load or offline mode, for each technology and FR interval. For other reserve sources, the table shows the fraction of the available reserve power that can be used in each interval.

	O_1^{dur} 1–5 s	O_2^{dur} 5–30 s	O_3^{dur} 30 s–5 min	O_4^{dur} 5–15 min	O_5^{dur} 15–30 min	O_6^{dur} 30–60 min
Power-to-heat	1	1	1	1	1	1
Curtailed VRE	1	1	1	1	1	1
Energy storage						
Li-ion battery	1	1	1	1	1	1
Hydrogen	1	1	1	1	1	1
Flywheels	1	1	1	1	1	1
Hydropower	0	0.15	0.3	1	1	1
Online thermal plants						
CCGT	0	0.0125	0.075	0.75	1	1
OCGT	0	0.1	0.3	1	1	1
ST	0	0.025	0.05	0.2	0.6	1
Nuclear	0	0	0	0.375	1	1
Offline thermal plants						
CC GT	0	0	0	0	0	0
OC GT	0	0	0	0	1	1
ST	0	0	0	0	0	0
Nuclear	0	0	0	0	0	0

CCGT: combined-cycle gas turbine; OCGT: open cycle gas turbine; ST: steam turbine.

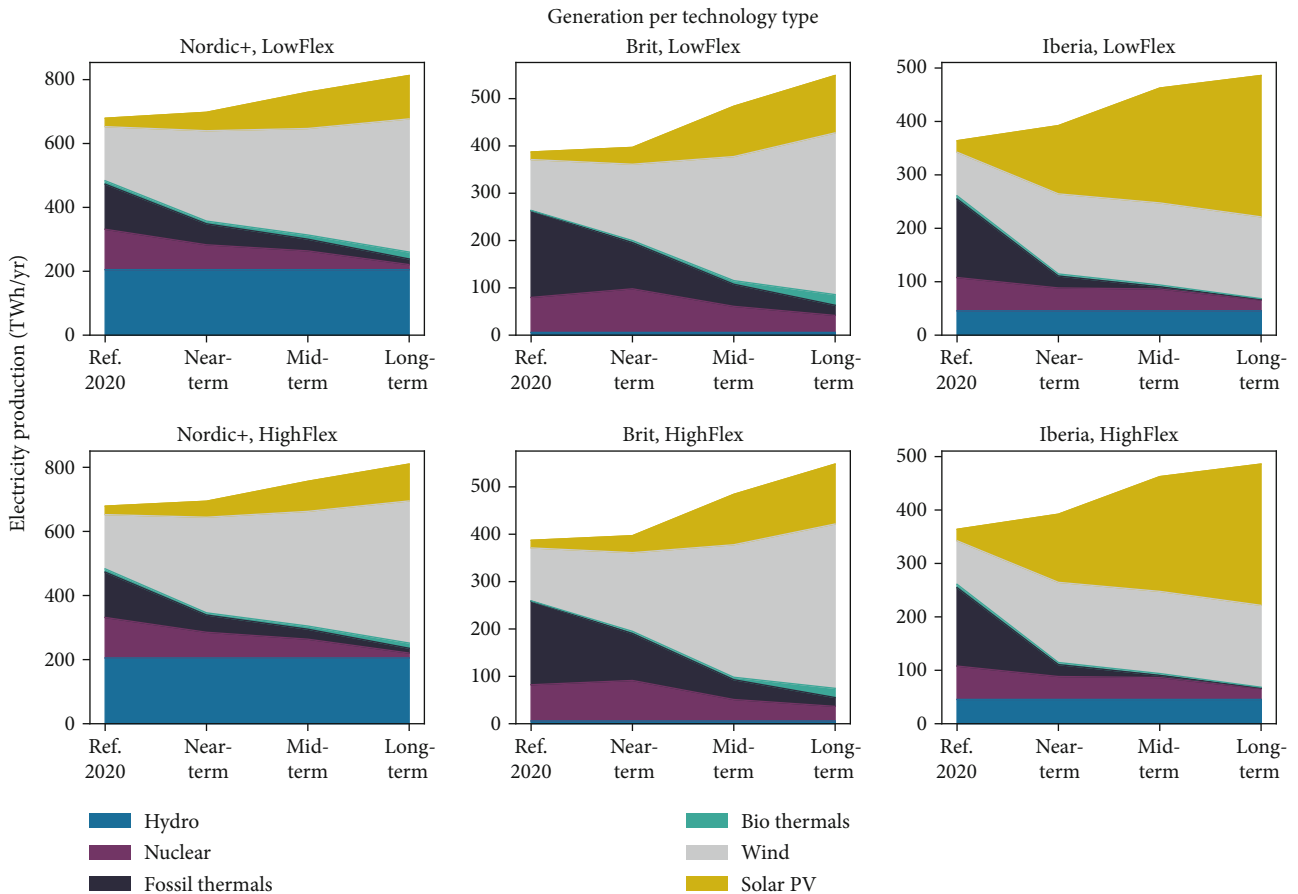


FIGURE 4: Yearly electricity supply development from the year 2020 to the long-term future for each generation technology type in each geographic region and system flexibility scenario, in the absence of any frequency control constraints.

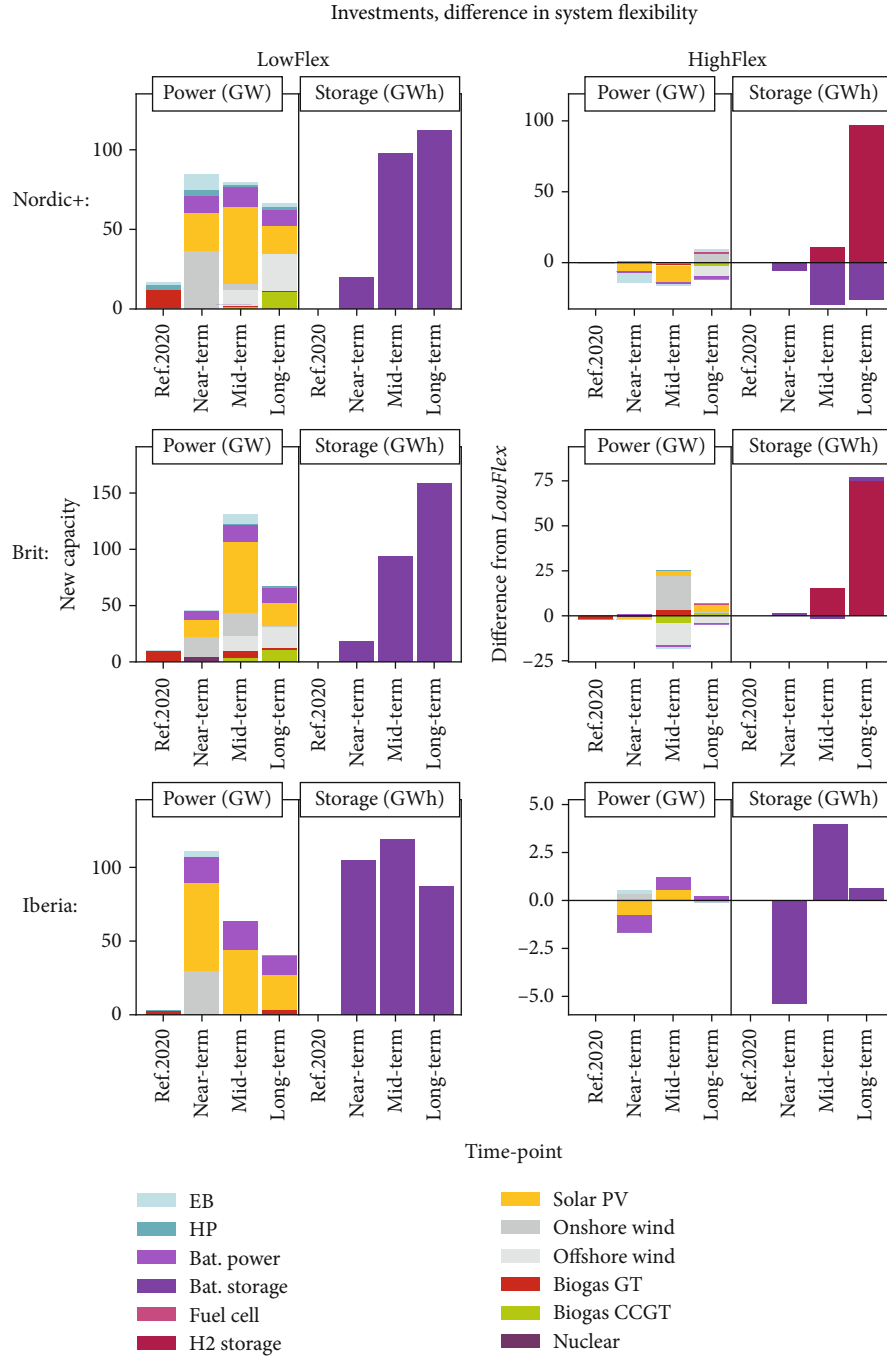


FIGURE 5: Installed capacities of power generation (GW) and storage (in GWh) for each year and scenario. Note the different y-axis for the subplots on the right-hand side.

remains unchanged in the two flexibility scenarios despite investments in hydrogen storage due to a lack of reservoir hydropower or other technologies that can manage shorter variations. In solar-dominated *Iberia*, the relatively low wind share and available reservoir hydropower result in no hydrogen storage investments being made in the *High-Flex* scenario. In addition, new transmission capacity has a limited impact on the system composition, as seen in Figure 4.

3.2. *Reserve Demand*. The reserve demand considered in this work consists of stochastic load variations, a dimensioning fault, and interhourly variations from wind and solar power generation. The box plot in Figure 6 illustrates the total reserve demand for each region and the time-point of the transition for the slow, 30–60-minute reserve category, during which the reserve demand is the highest. This shows that while the number of high-demand hours increases along with the reserve demand during these hours, the median

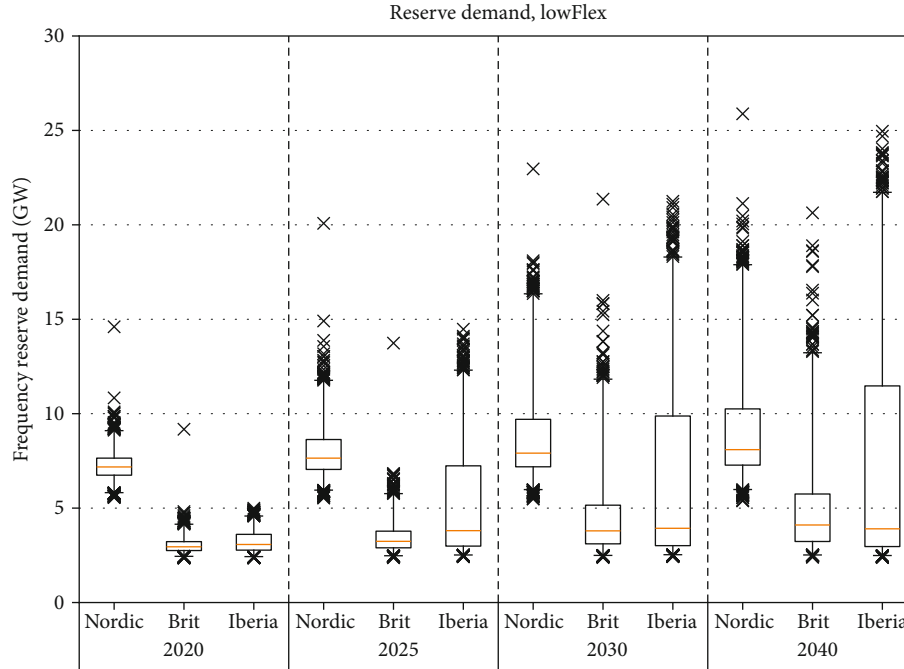


FIGURE 6: Box plot of the total reserve demand for each region and time-point of the transition, for the 30–60-minute reserve interval. The orange bar indicates the median, each box spans from the 1st to the 3rd quartile, and the whiskers extend to the 1st and 99th percentiles, with the crosses indicating data points outside the 1st to 99th percentiles.

reserve is increased only slightly. For reference, the dimensioning fault and average stochastic load variations amount to 1.8, 0.4, and 0.4 GW in the *Nordic+*, *Brit*, and *Iberia* regions, respectively. This means that most of the reserve demand originates from the ramping of the VRE output.

3.3. Reserve Supply. In Table 8, the total reserve market size is approximated by the sum of the marginal costs for each reserve interval and each hour, multiplied by the reserve demand. A clearly evident trend in Table 8 is the decrease in reserve market size over time, especially between the Ref. 2020 and the near-term time-points. This trend is contrary to the demand for reserves which, as illustrated in Figure 6, slightly increases over time. The decrease in market size is largely due to less reserves being supplied by thermal power, which must run at part-load and, as a consequence, incurs a direct cost to make reserves available (regardless of whether the reserves are needed). In the Ref. 2020 time-point, before storage investments are possible, there are less alternative sources of reserves. Table 8 also highlights significant differences in market size between the regions, with *Iberia* having significantly lower total revenue than *Nordic+* and *Brit*. As shown in Figure 4, *Nordic+* and *Iberia* have more hydropower than the *Brit* region. Both access to hydropower and reserve demand sources explain the differences in reserve market size between the regions. The reserve demand has a different profile in *Iberia* due to the higher share of solar power. The rapid changes in solar power during the morning and evening concentrate much of the reserve demand to these hours. If low-cost reserve suppliers, such as storage units or hydropower, are available during

TABLE 8: Total reserve market size (M€/yr) for each region, transition time-point, and flexibility scenario.

	M€/yr	Ref. 2020	Near-term	Mid-term	Long-term
LowFlex	Nordic+	126	20	14	7
	Brit	118	11	8	5
	Iberia	41	0.4	0.2	1
HighFlex	Nordic+	171	21	17	8
	Brit	133	14	9	2
	Iberia	42	0.4	0.0	2

these high-reserve hours, the reserve market price and, thus, the revenue from providing reserves decrease.

The technologies used to supply the reserves are illustrated in Figure 7 for the *LowFlex* and *HighFlex* scenarios in the upper and lower rows of panels, respectively. In this figure, the share of the total reserve supply is shown as bars on the left y-axis, while the reserve market size is shown as rhombs on the right y-axis. The reserve shares show some of the differences between the regions in terms of access to hydropower, usage of thermal power plants for reserves, and the possibility of using power-to-heat in district heating networks. For example, even though the *Nordic+* region has a higher share of electricity supplied from hydropower than the *Iberia* region, *Iberia* has about twice the share of the reserves from hydropower compared to *Nordic+*. As previously mentioned in Table 8, this implies that hydropower is often available to provide reserves during the hours when the solar PV output varies the most (late mornings and afternoons) in the *Iberia* region.

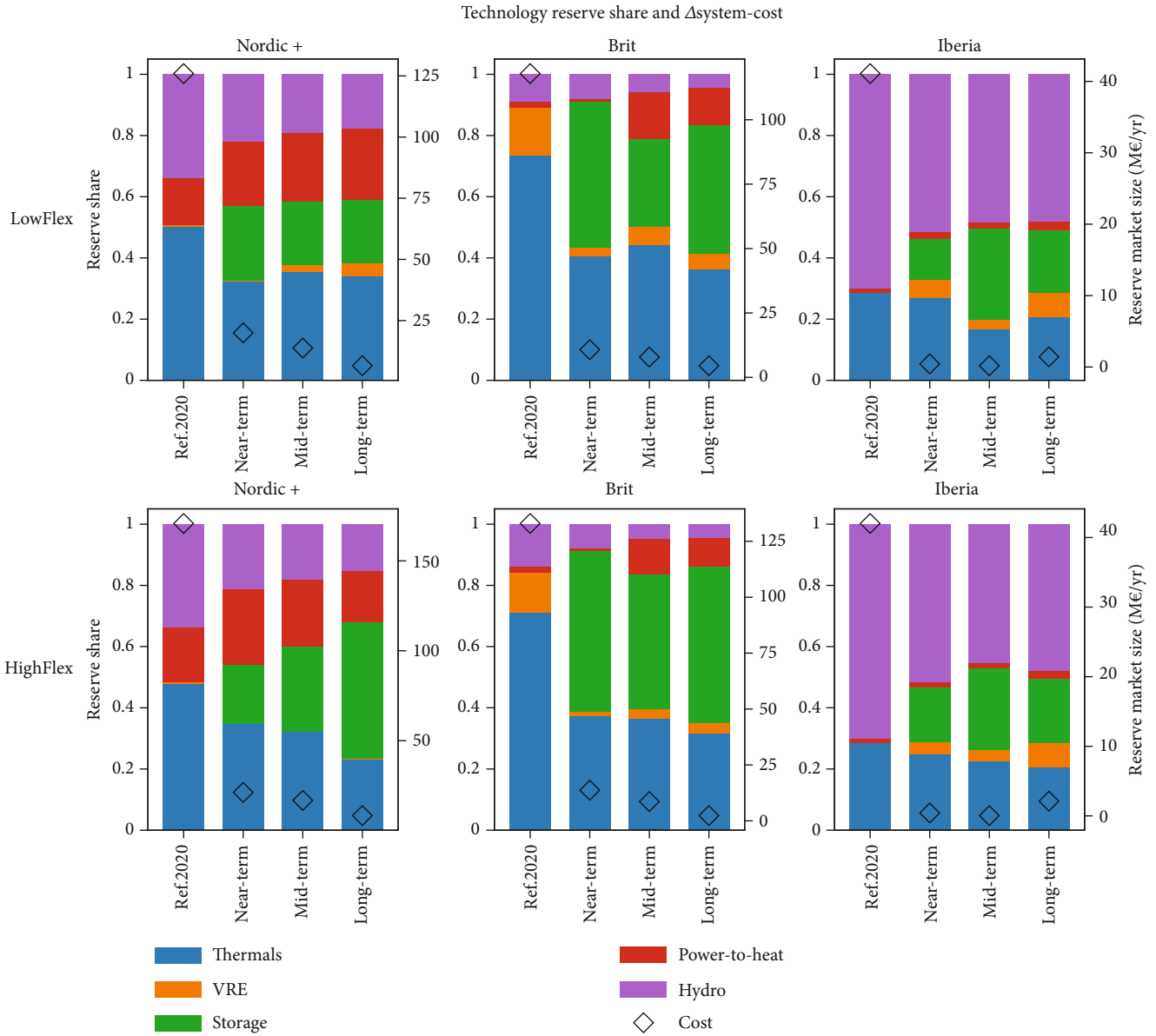


FIGURE 7: Reserve shares per technology (left-hand y -axis) for each year and region in the LowFlex scenarios. The rhombic symbols indicate the reserve market size, expressed as the marginal cost of reserves multiplied by the reserve demand, summed over each hour and interval (right-hand y -axis).

In Figure 8, the potential revenues from supplying the reserve demand are shown, per installed capacity, as lines for each region and flexibility scenario. The dotted lines marked with H represent the potential revenues in the *HighFlex* scenarios, and the solid lines marked with L represent the potential revenues in the *LowFlex* scenarios. This shows that while batteries account for only a fraction of the reserve supply once investments are allowed (as seen in Figure 7), the addition of new low-cost reserves and the corresponding reduction in the reserve market size also reduce the potential revenue from supplying reserves from thermal and hydro-power. Further along the transition, in the mid-term and long-term scenarios, the revenue per installed capacity falls as more and more batteries are invested in for hour-to-

hour variation management. The shift towards batteries for hour-to-hour variation management also decreases the reserve prices, since the availability of reserves from batteries does not directly incur increased costs.

In terms of the share of each technology's total revenue, the reserve supply revenue is $\leq 1\%$ for almost every region, time-point of the transition, and flexibility scenario (for more details, see Table 9 in the Appendix). The exceptions to this are power-to-heat in the Ref. 2020 time-point and batteries in the near-term period. For batteries in the near term, the revenue shares from supplying reserves could be 6%–10% in the *Nordic+* case and anywhere in the range of 4%–100% (4% in *LowFlex* and 100% in *HighFlex*) in the *Brit* case. For power-to-heat in the Ref. 2020 time-point, the

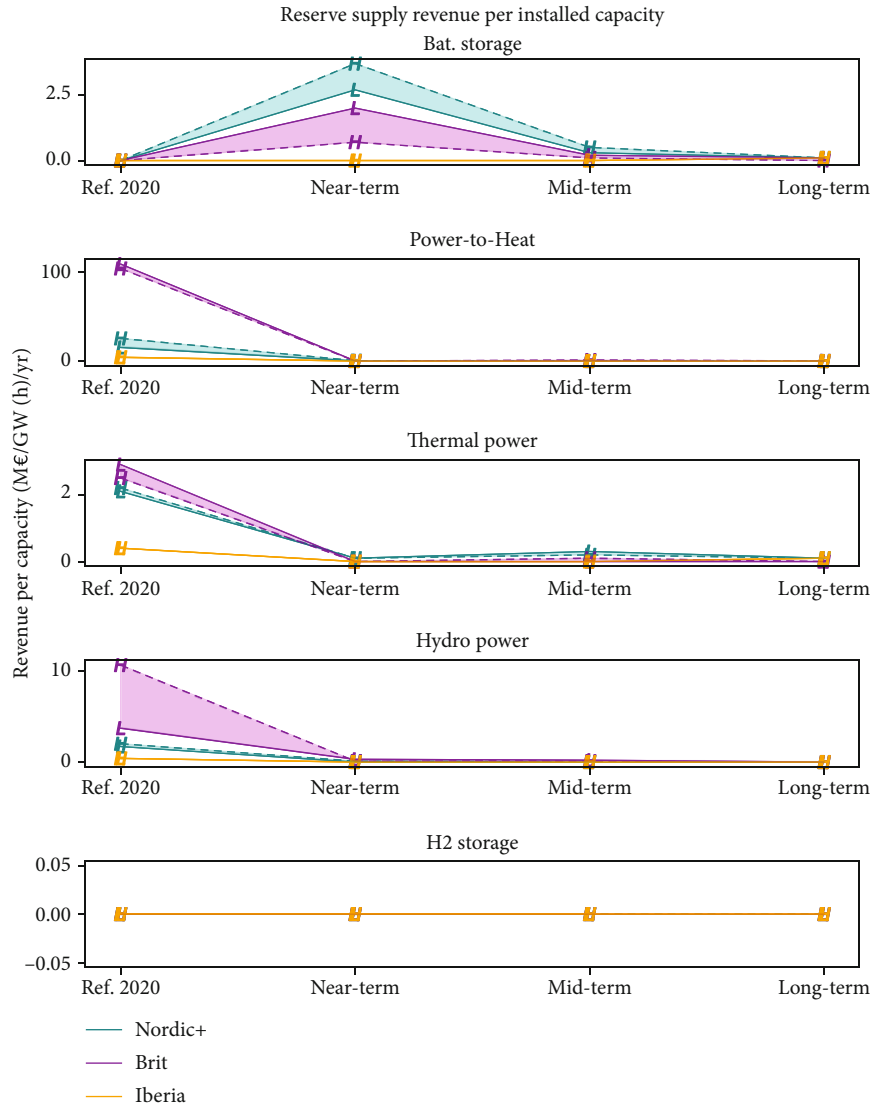


FIGURE 8: Revenue from supplying frequency reserves for batteries, power-to-heat (HPs and EBs) units, and thermal power plants in the three geographic cases and for the LowFlex and HighFlex scenarios.

revenue share could be 8%–11% in the *Nordic+* case and 91% in the *Brit* case. The high shares are seen only when the respective installed capacities (and thus, the revenues) from electricity supply are small, but also in the early stages of the transition when fewer batteries and flexible loads are available.

4. Discussion

The model applied in this work uses load and weather profiles from the year 2012, in combination with current and future projections of electricity loads. The frequency control implementation estimates the reserve demand and ensures that sufficient reserves are available to meet the demand, if needed. This modeling gives insights into cost-effective means to provide reserves and inertia in different contexts, as well as the relative importance levels of various technologies. However, without accurate knowledge as to how much of the reserves will have to be *activated* each hour, the reve-

nues from supplying such reserves can only be estimated using the available reserves from each technology and the marginal cost of providing reserves. The real revenues will depend on the reserve market structure, which could compensate suppliers for activated reserves, available reserves, or both. The compensation structure might similarly differ from the one assumed in this work, compensating suppliers of reserves according to their own bid (pay-as-bid) instead of using the marginal cost of supply. For reference, the current reserve market structure in Sweden compensates all suppliers of fast reserves (FFR) and frequency restoration reserves (FRR) according to the highest accepted bid, regardless of activation calls. The other type of reserves, frequency containment reserves (FCR), is currently pay-as-bid but is transitioning to the highest accepted bid in the year 2024 [37]. In reality, the revenues will depend on the actual development of the electricity system, subject to policy decisions and local actors.

TABLE 9: Shares of total revenue coming from reserve supplies for batteries, power-to-heat, thermal power, hydropower, and hydrogen storage systems (electrolyzers and fuel cells).

%	Battery	PtH	Thermal	Hydro	H ₂ storage
<i>Nordic+</i>					
Ref. year 2020	0/0	8/11	1/1	0/1	0/0
Near-term	6/10	0/0	0/0	0/0	0/0
Mid-term	1/2	0/0	0/0	0/0	0/0
Long-term	1/1	0/0	0/0	0/0	0/0
<i>Brit</i>					
Ref. year 2020	0/0	91/91	1/1	3/7	0/0
Near-term	4/100	1/1	0/0	0/0	0/0
Mid-term	1/0	0/3	0/0	0/0	0/0
Long-term	0/0	0/0	0/0	0/0	0/0
<i>Iberia</i>					
Ref. year 2020	0/0	1/2	0/0	0/0	0/0
Near-term	0/0	0/0	0/0	0/0	0/0
Mid-term	0/0	0/0	0/0	0/0	0/0
Long-term	0/1	0/0	0/0	0/0	0/0

PtH: power-to-heat.

Factors that may underestimate the reserve price as obtained in this work and, in turn, the market size include the assumptions on perfect foresight, no battery degradation, a perfect market (perfect information and no bid markup above the marginal cost of supply), and no activation of the reserves. The latter means that there is no impact on heat or storage balance and no increased fuel use when activating the thermal power reserves. At the same time, the following factors act in the opposite direction, i.e., overestimating the reserve price and market size: the assumed reserve demand is on the high end (e.g., 7 GW for Nordic+, Ref. 2020), some potential demand-side reserve suppliers are omitted, and all compensation is assumed to follow the highest accepted bid instead of pay-as-bid. Combined, the net impact is likely an underestimation of the reserve prices and market size for all stages of the modeled energy transition. Similarly, the reduction in reserve prices and market size over time (100-fold reduction in Iberia between Ref. 2020 and the near-term time-point) found in this work may be exaggerated. It is, however, not unrealistic that a transition to investment-based reserve sources with a low marginal cost of supply decreases the reserve prices significantly, especially when another market drives the investments. Still, too low compensation to reserve suppliers may cause potentially available reserves to be withheld, especially from small-scale consumers and households. This could, in turn, increase the cost of reserves to some level where a sufficient number of potential reserve providers are motivated to participate. This effect is not captured in this work. In summary, while the reserve prices and market sizes found in this work may be underestimated, the trends and general figures found should not be unreasonable.

As electricity systems transition towards high shares of variable electricity generation and society transitions

towards greater electrification and smarter devices, it may be of interest to employ new technologies to provide reserves and/or inertia to the grid. This might include the use of battery electric vehicles, residential or centralized heat pumps and electric boilers (Herre et al. [38] have found that, in Sweden, residential electric heating alone can deliver reserves averaging 2 GW/0.1 Hz over the year.), electrolyzers, and thermostatically controlled loads such as air-conditioned server halls or refrigerated spaces. While all of these examples have a different primary purpose, they could assist in maintaining grid stability at low to no cost (without significantly impeding their main purpose), assuming that they are required or sufficiently incentivized to do so. All the listed new reserve technologies have rapid reaction times (with electrolyzers being the slowest technology, requiring more than 1 second to adjust the output), albeit of limited duration. The model applied in this work includes power-to-heat and electrolyzers, under the assumption that they contribute fully to the reserve supply when possible. The model does, however, only consider hydrogen-to-electricity through fuel cells, of which no investments were part of the cost-optimal solution. Hydrogen gas turbines may be a more cost-competitive technology [23], though it is unlikely that hydrogen gas turbines would affect the results in this work since biogas turbines are included in the model. Not including also other demand-side technologies is done to limit the scope of the work, and since the value (and thus, the incentive to participate in flexibility markets) declines as more technologies make contributions. For example, including reserves from battery electric vehicles in the model eliminates the cost impact from the reserve and inertia demand owing to the availability of large battery capacity. Even if allowed by the grid code, the use of these technologies for reserves would, in reality, be limited by the reserve demand and the level of compensation granted for available and/or activated reserves. The inclusion of additional demand-side frequency control technologies may thus not result in a better representation unless the compensation required to achieve participation is known. Still, a technology-neutral grid code that enables contributions from these technologies could be important for minimizing the cost of supplying the reserve demand. It should also be noted that there is additional value, although hard to quantify, in having a larger supply of frequency control than is strictly necessary. In the case of an emergency (such as a natural disaster or war), additional frequency control supply may be necessary to compensate for lost supply. Due to the modularity as well as the large power and storage capacity found for grid-scale batteries, a grid that integrates batteries (and other inverter-based sources) into the reserve and inertia supply may be more resilient to future developments which will have increased requirements on the demand for reserves and/or inertia. In addition, the grid code and technology implementation used to aggregate and incorporate decentralized converter-based reserve sources (such as batteries, wind power, and solar PV) opens the door to a larger group of potential frequency control devices on the demand side.

The reserve market sizes listed in Table 8, which are based on the cost for reserve *availability*, indicate the

differences in market size between the regions and as the electricity systems transition. For example, the reserve market size for the Nordic region is 126–170 M€ for the dispatch-only year 2020. The real cost of FCR-N, FCR-D, and aFRR in Sweden in 2021 was roughly 323 M€. Despite Sweden only making up around 22% of the Nordic+ electricity demand in the modeled year 2020, the real reserve market size for Sweden is about twice that of the whole Nordic+ region. The discrepancy between the modeled market and the real market in terms of costs is attributed to reserve activation. While the model only requires that reserves be available, imbalances in the real system result in the activation of reserves, incurring additional fuel costs. In the real system, there are also regulatory limitations on the supply as well as limited participation from power-to-heat, wind power, and solar PV installations. As such, conclusions drawn regarding the market sizes are limited to the differences in market size between regions and between the transition stages. The drastic decline in reserve prices in the short term is due to the addition of flexibility technologies, such as batteries and power-to-heat or power-to-hydrogen units with storage. This reduces the cost of reserve availability because these flexible technologies, unlike thermal power plants, do not need to incur part-load costs. The cost of activating reserves from these technologies can also be very low if spare capacity is available, and the storage level can be restored by providing symmetrical down-reserves before the battery is scheduled to be fully discharged.

To the degree that the results in this study can be compared to those found by van Stiphout et al. [30] and González-Inostroza et al. [26], they seem to find similar results as in this work and their conclusions complement the ones drawn in previous studies. van Stiphout et al. find that allowing wind and solar power to supply reserves decreases the system cost and the amount of reserves originating from thermal power. Similarly, the results in this work show that the amount of reserves from thermal power decreases as the VRE share increases. González-Inostroza et al. conclude that battery participation appears to be a cost-efficient solution to the increased demand for fast frequency reserves in renewable future electricity systems. The findings in this work also indicate that batteries could play a large role in the future of grid frequency control.

5. Conclusions

To fill the gap in research about reserve market sizes and drivers for investments in technologies providing grid frequency control, this study combines electricity capacity expansion modeling with a representation of grid frequency control supply and demand. In doing so, this study investigates how the frequency control reserve market may change as electricity systems move towards increasing shares of inverter-based wind and solar PV power. Results are presented that show the electricity supply and technology mix for each region and time-point in the transition, how the demand for reserves evolves, as well as how the reserve is

supplied. Also presented is the total reserve market size, as well as which technologies will benefit the most from reserves. However, due to limitations in scope and representation of real-world circumstances (such as energy policies and market structures), the reserve market sizes and revenues obtained in this work may be underestimated, as discussed in Section 4. The following conclusions are drawn:

- (i) Deployment of grid-scale batteries in the near-term can drastically reduce the reserve market size by reducing the cost of reserve availability
- (ii) For most technologies, stages of the transition, and regions, revenue from reserve markets is insufficient to drive significant additional investments. Some exceptions can be seen for the use of batteries in the near-term, depending on system flexibility, and the use of power-to-heat if battery investments are delayed

As these findings indicate that there may be large changes in the market sizes and revenues afforded to frequency reserve suppliers in the near-term, there is a need for future work that further investigates this topic. Specifically, factors that affect the market development and indicators that can be used to predict the market changes may be of great value. Knowledge of the minimum compensation for participation from household consumers may also become increasingly valuable.

Appendix

Supplementary Results

The share of total revenue coming from supplying reserves, for each technology type, time-point of the transition, regional case, and flexibility scenario, is shown in Table 9. With only a few exceptions, the revenue share from providing reserves generally is negligible. The exceptions to this are Ref. year 2020 and batteries in the near-term.

Data Availability

The input files used to support the findings of this study are available from the corresponding author upon request.

Conflicts of Interest

The authors declare that they have no known competing financial interests or personal relationships that could have influenced the work reported in this paper.

Acknowledgments

The project has been funded by the Swedish Energy Agency (44986-1). Open Access funding was enabled and organized by Bibsam 2023.

References

- [1] M. Merten, F. Rücker, I. Schoeneberger, and D. U. Sauer, "Automatic frequency restoration reserve market prediction: methodology and comparison of various approaches," *Applied Energy*, vol. 268, article 114978, 2020.
- [2] F. Nitsch, M. Deissenroth-Uhrig, C. Schimeczek, and V. Bertsch, "Economic evaluation of battery storage systems bidding on day-ahead and automatic frequency restoration reserves markets," *Applied Energy*, vol. 298, 2021.
- [3] M. Merten, C. Olk, I. Schoeneberger, and D. U. Sauer, "Bidding strategy for battery storage systems in the secondary control reserve market," *Applied Energy*, vol. 268, 2020.
- [4] J. Badeda, J. Meyer, and D. U. Sauer, "Modeling the influence of installed battery energy storage systems on the German frequency containment reserve market," in *NEIS 2017; Conference on Sustainable Energy Supply and Energy Storage Systems*, pp. 315–321, Hamburg, Germany, 2020, <https://ieeexplore.ieee.org/document/8421832>.
- [5] A. Boldrini, J. P. Jiménez Navarro, W. H. J. Crijs-Graus, and M. A. van den Broek, "The role of district heating systems to provide balancing services in the European Union," *Renewable and Sustainable Energy Reviews*, vol. 154, 2020.
- [6] X. Li, X. Yu, and Z. Gao, "Research on the optimal strategy of pumped storage power station to provide multiple time-scale reserves," *Journal of Physics: Conference Series*, vol. 2108, no. 1, 2021.
- [7] A. Roos and T. F. Bolkesjø, "Value of demand flexibility on spot and reserve electricity markets in future power system with increased shares of variable renewable energy," *Energy*, vol. 144, pp. 207–217, 2018.
- [8] J. Seidel, F. Rauscher, and B. Engel, "Enhanced contribution of photovoltaic power systems to frequency control in future power systems," *IET Renewable Power Generation*, vol. 15, no. 12, pp. 2753–2765, 2021.
- [9] F. Braeuer, J. Rominger, R. McKenna, and W. Fichtner, "Battery storage systems: an economic model-based analysis of parallel revenue streams and general implications for industry," *Applied Energy*, vol. 239, pp. 1424–1440, 2019.
- [10] P. Fernández-Bustamante, O. Barambones, I. Calvo, C. Napole, and M. Derbeli, "Provision of frequency response from wind farms: a review," *Energies*, vol. 14, no. 20, p. 6689, 2021.
- [11] J. Figgner, B. Tepe, F. Rücker et al., "The influence of frequency containment reserve flexibilization on the economics of electric vehicle fleet operation," *Journal of Energy Storage*, vol. 53, article 105138, 2022.
- [12] R. Hollinger, L. M. Diazgranados, and T. Erge, "Trends in the German PCR market: perspectives for battery systems," in *2015 12th International Conference on the European Energy Market (EEM)*, Lisbon, Portugal, 2015.
- [13] S. Huclin, J. P. Chaves, A. Ramos et al., "Exploring the roles of storage technologies in the Spanish electricity system with high share of renewable energy," *Energy Reports*, vol. 8, pp. 4041–4057, 2022.
- [14] B. Illing and O. Warweg, "Achievable revenues for electric vehicles according to current and future energy market conditions," in *2016 13th International Conference on the European Energy Market (EEM)*, Porto, Portugal, 2016.
- [15] A. Khazali and M. Kalantar, "Optimal dispatch of responsive loads and generic energy storage units in a co-optimized energy and reserve market for smart power systems," *Electric Power Components and Systems*, vol. 44, no. 20, pp. 2285–2297, 2016.
- [16] B. Kladnik, G. Artac, T. Stokelj, R. Golob, and A. F. Gubina, "Demand-side participation in system reserve provision in a stochastic market model with high wind penetration," in *2012 IEEE International Conference on Power System Technology (POWERCON)*, Auckland, New Zealand, 2012.
- [17] N. E. Koltsaklis and A. S. Dagoumas, "State-of-the-art generation expansion planning: a review," *Applied Energy*, vol. 230, pp. 563–589, 2018.
- [18] H. K. Ringkjøb, P. M. Haugan, and I. M. Solbrekke, "A review of modelling tools for energy and electricity systems with large shares of variable renewables," *Renewable and Sustainable Energy Reviews*, vol. 96, pp. 440–459, 2018.
- [19] N. Helistö, J. Kiviluoma, H. Holttinen, J. D. Lara, and B. M. Hodge, "Including operational aspects in the planning of power systems with large amounts of variable generation: a review of modeling approaches," *Wiley Interdisciplinary Reviews: Energy and Environment*, vol. 8, no. 5, article e341, 2019.
- [20] M. Taljegard, L. Göransson, M. Odenberger, and F. Johnsson, "To represent electric vehicles in electricity systems modelling—aggregated vehicle representation vs. individual driving profiles," *Energies*, vol. 14, no. 3, p. 539, 2021.
- [21] V. Walter and L. Göransson, "Trade as a variation management strategy for wind and solar power integration," *Energy*, vol. 238, p. 121465, 2022.
- [22] L. Tuan, M. Q. Duong, G. N. Sava, and V. Tanasiev, "Optimization of renewable energy sources operation in Vietnam's electricity market," *Rev Roumaine des Sciences Techniques-Series Electrotechnique et Energetique*, vol. 65, no. 3–4, pp. 221–227, 2020, http://revue.elth.pub.ro/upload/44519912_MDuong_RRST_3-4_2020_pp_221-227.pdf.
- [23] S. Öberg, M. Odenberger, and F. Johnsson, "The cost dynamics of hydrogen supply in future energy systems - a techno-economic study," *Applied Energy*, vol. 328, article 120233, 2022.
- [24] Z. Wang, J. Wang, G. Li, and M. Zhou, "Generation-expansion planning with linearized primary frequency response constraints," *Global Energy Interconnection*, vol. 3, no. 4, pp. 346–354, 2020.
- [25] C. Zhang, L. Liu, H. Cheng et al., "Frequency-constrained generation expansion planning with frequency support from wind farm," in *2020 IEEE/IAS Industrial and Commercial Power System Asia (I&CPS Asia)*, pp. 668–674, Weihai, China, 2020.
- [26] P. González-Inostroza, C. Rahmann, R. Álvarez, J. Haas, W. Nowak, and C. Rehtanz, "The role of fast frequency response of energy storage systems and renewables for ensuring frequency stability in future low-inertia power systems," *Sustainability*, vol. 13, no. 10, p. 5656, 2021.
- [27] S. T. P. Løvengreen, *Security-constrained expansion planning of low carbon power systems*, Melbourne School of Engineering, 2021.
- [28] Y. Tanoto, I. MacGill, A. Bruce, and N. Haghdadi, "Impact of high solar and wind penetrations and different reliability targets on dynamic operating reserves in electricity generation expansion planning," *The Electricity Journal*, vol. 34, no. 4, article 106934, 2021.
- [29] T. Brijs, A. van Stiphout, S. Siddiqui, and R. Belmans, "Evaluating the role of electricity storage by considering short-term operation in long-term planning," *Sustainable Energy, Grids and Networks*, vol. 10, pp. 104–117, 2017.

- [30] A. van Stiphout, K. De Vos, and G. Deconinck, "The impact of operating reserves on investment planning of renewable power systems," *IEEE Transactions on Power Apparatus and Systems*, vol. 32, no. 1, pp. 378–388, 2017.
- [31] J. Ullmark, L. Göransson, and F. Johnsson, "Frequency reserves and inertia in the transition to future electricity systems," *Energy Systems*, pp. 1–34, 2023.
- [32] J. Ullmark, *Optimization modeling of frequency reserves and inertia in the transition to a climate-neutral electricity system*, Chalmers University of Technology, 2023.
- [33] L. Göransson, J. Goop, M. Odenberger, and F. Johnsson, "Impact of thermal plant cycling on the cost-optimal composition of a regional electricity generation system," *Applied Energy*, vol. 197, pp. 230–240, 2017.
- [34] V. Johansson and L. Göransson, "Impacts of variation management on cost-optimal investments in wind power and solar photovoltaics," *Renewable Energy Focus*, vol. 32, pp. 10–22, 2020.
- [35] C. Weber, *Uncertainty in the Electric Power Industry*, vol. 77, Springer New York, New York, NY, 2005.
- [36] P. Imgart and P. Chen, "Evaluation of the system-aggregated potentials of inertial support capabilities from wind turbines," in *2019 IEEE PES Innovative Smart Grid Technologies Europe (ISGT-Europe)*, Bucharest, Romania, 2019.
- [37] SVK, "Introduction of marginal pricing on FCR markets," <https://www.svk.se/en/about-us/news/news/introduction-of-marginal-pricing-on-fcr-markets/>.
- [38] L. Herre, B. Nourozi, M. R. Hesamzadeh, Q. Wang, and L. Söder, "A bottom-up quantification of flexibility potential from the thermal energy storage in electric space heating electric power rating time a TCL takes in powered mode from one end of the deadband to the other time a TCL takes in unpowered mode from one end," 2021 <https://orbit.dtu.dk/en/persons/lars-finn-herre>.